LGAD Development at Teledyne e2v for the LHC's High-Luminosity (HL) Upgrade

38th RD50 Workshop, 22 June 2021

M. Gazi, D. Bortoletto, R. Plackett, E. G. Villani, S. McMahon, J. Mulvey, I. Kopsalis, P. Allport, L. Gonella, K. Stefanov, D. Jordan

Science & Technology Facilities Council
Rutherford Appleton Laboratory

UNIVERSITY OF BIRMINGHAM

TELEDYNE e2v
Everywhereyoulook™

Outline

- Introduction: Ultra Fast Silicon Detectors
- Project overview: LGADs manufactured by Teledyne e2v
- LGAD Simulation
- Wafer characterization: IV and CV
- Inferred doping density
- Dicing and post-dicing treatment
- Summary

The need for Ultra Fast Silicon Detectors

- HL-LHC: Pile-up is one of the major challenges for tracking
- Detectors with high granularity for spatial measurement with added high resolution time measurement (4D tracking)
- Timing information used to disentangle overlapping events
- ATLAS High-Granularity Timing Detector placed outside the ITk

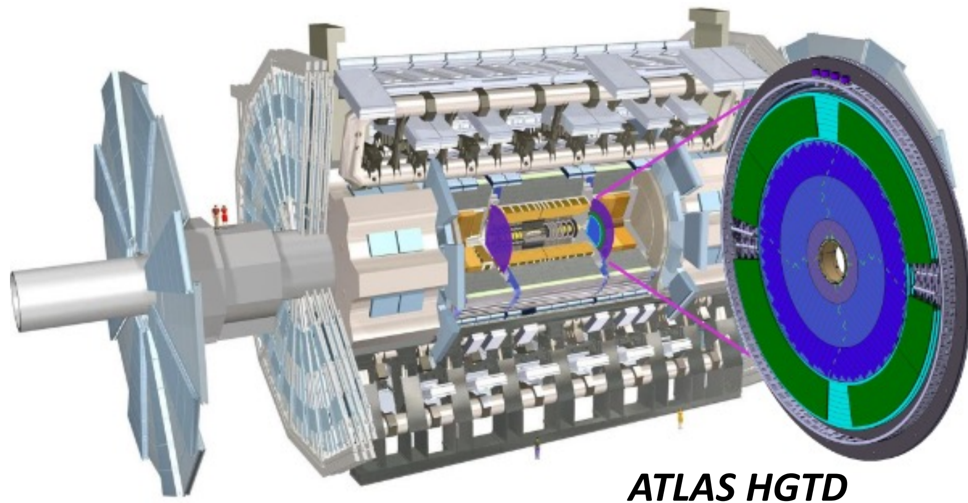

1 pp interaction amongst 200

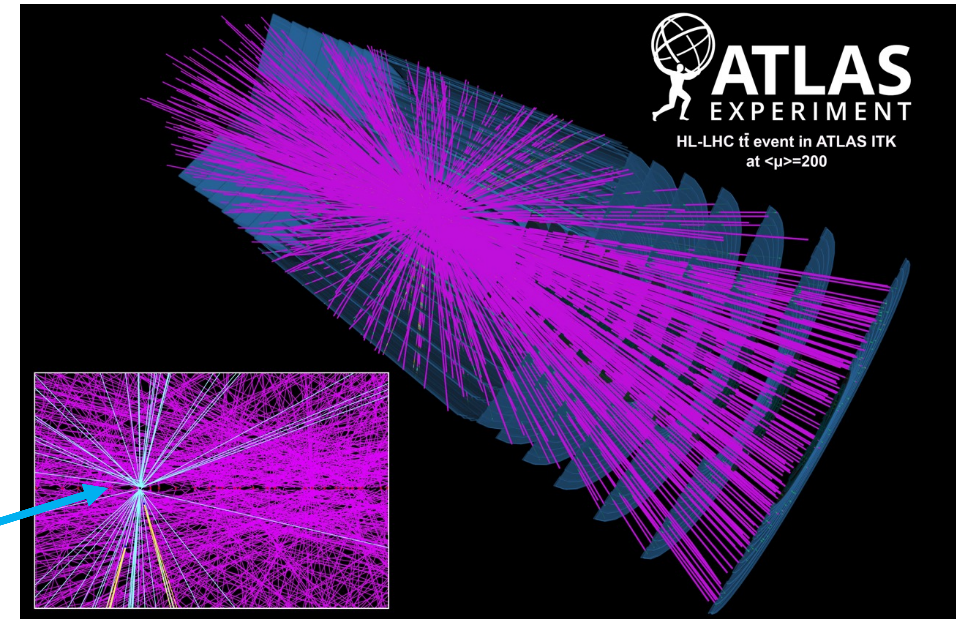

Low Gain Avalanche Detectors (LGAD)

- Aim: Track timing resolution of ≈30-50 ps over detector lifetime
- Boron implantation forms gain layer (p^+) -> impact ionization
- Time resolution of LGAD benefits from high slew rate, which is increased by introducing internal gain G

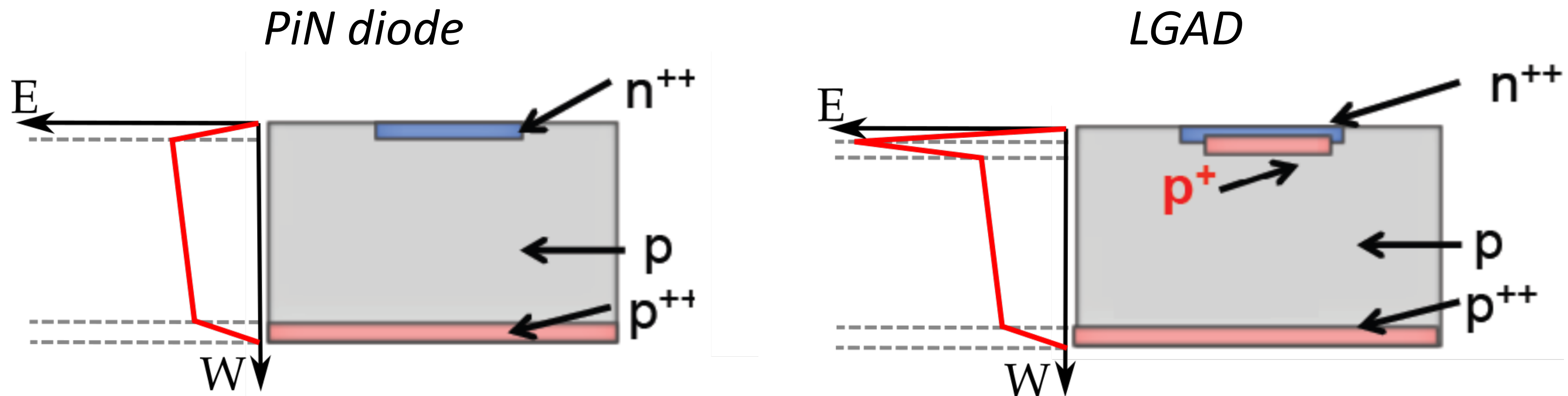

Teledyne e2v LGAD project

- Epitaxial layer: 50 um, high resistivity
- Boron as the gain layer dopant
  - 8 different combinations of manufacturing parameters
- Each field contains LGADs and PiN diodes of the same layout (4 mm, 2 mm, 1 mm)

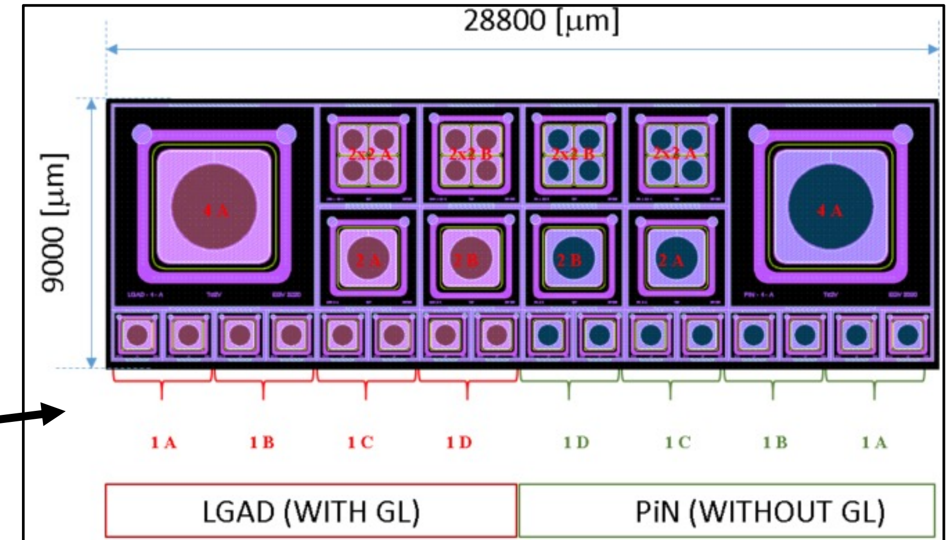

Wafer code	Implant dose (normalised)	Implant energy (normalised)
A	1.07	1.11
B	1.07	1.05
C	1.07	1.00
D	0.92	1.05
E	1.15	1.05
F	1.00	1.00
G	1.00	1.05
H	1.00	1.11

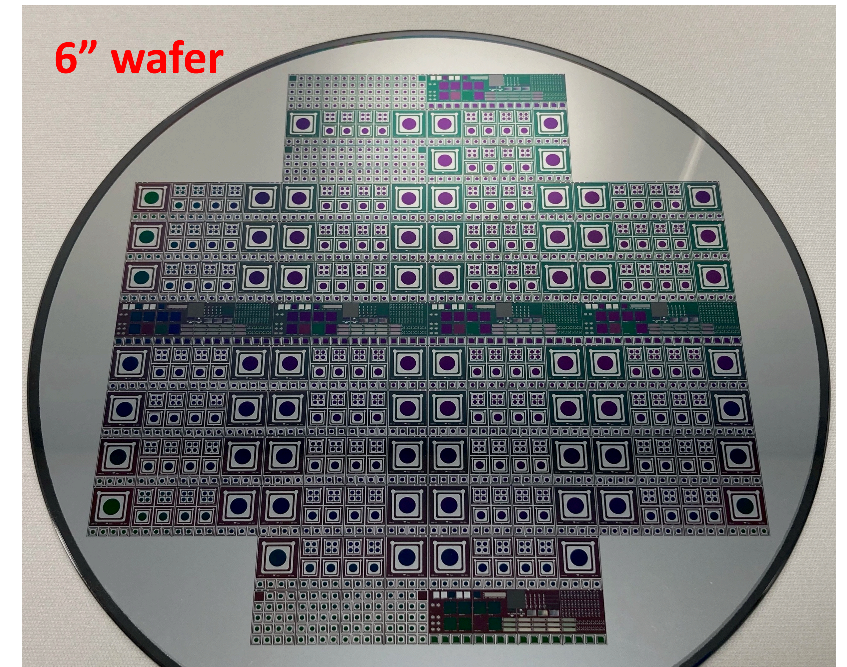

LGAD Simulation I

- Fabrication steps of the devices simulated using TCAD tool from Synopsis

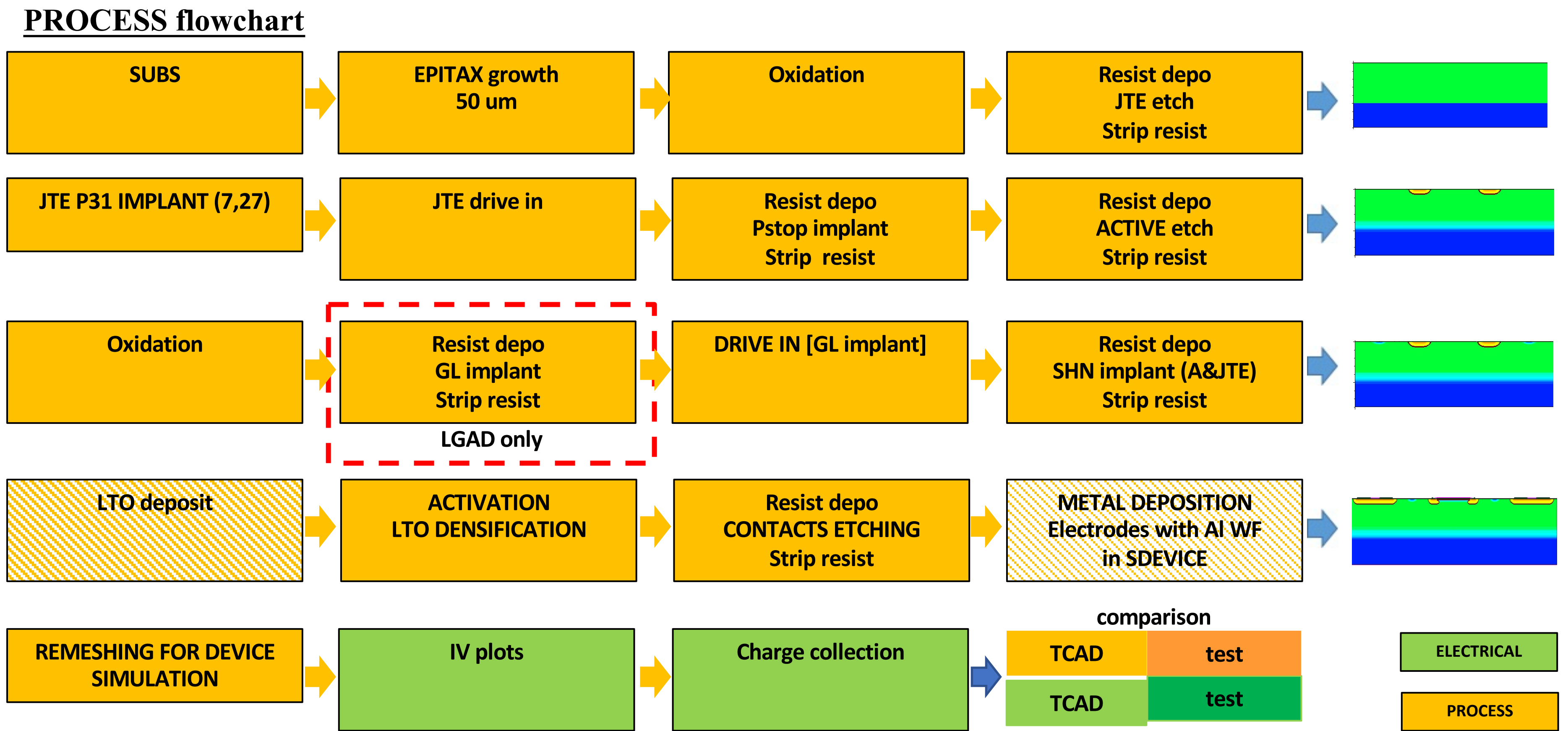

LGAD Simulation II

- Electrical simulation setup, common to PiN and LGAD, with RC network

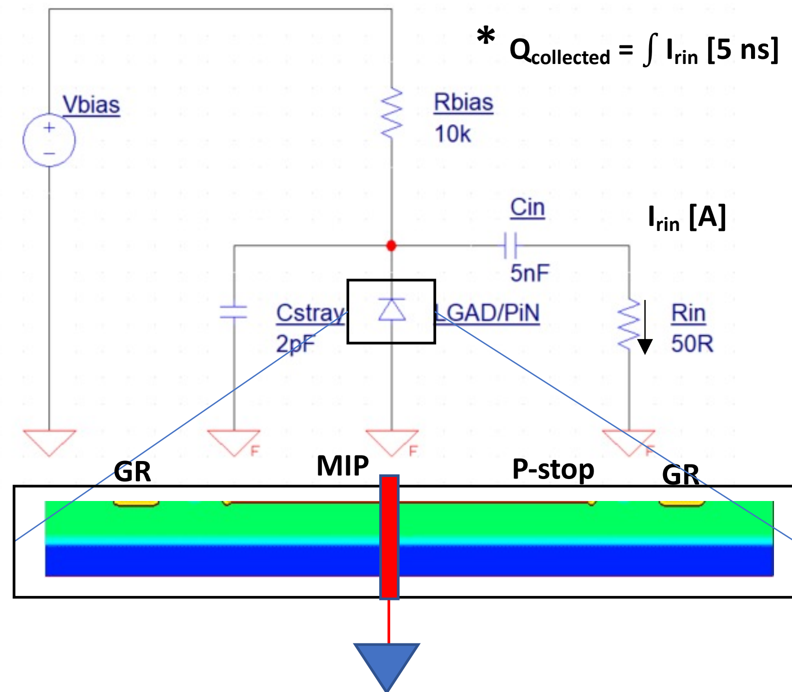

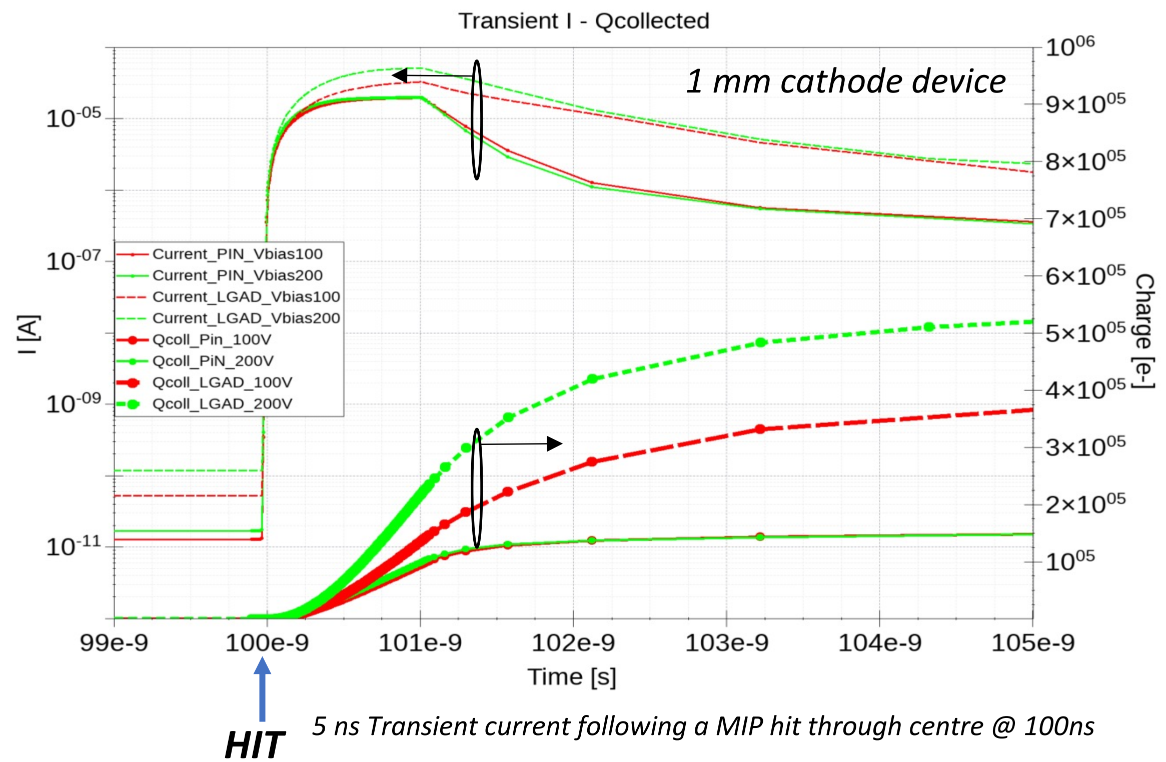

5 ns Transient current following a MIP hit through centre @ 100ns

- Bulk radiation damage not included in this iteration, but effects of $Si\text{-}SiO_2$ surface states have been modelled

Wafers of interest

- Variation of behaviour with implant energy (dose constant)

Wafer code	Implant dose (normalised)	Implant energy (normalised)
A	1.07	1.11
B	1.07	1.05

Parameters normalised to a reference dose and energy of the implant

Measured 5 LGADs and 5 PiNs

(consistent colour coding used throughout)

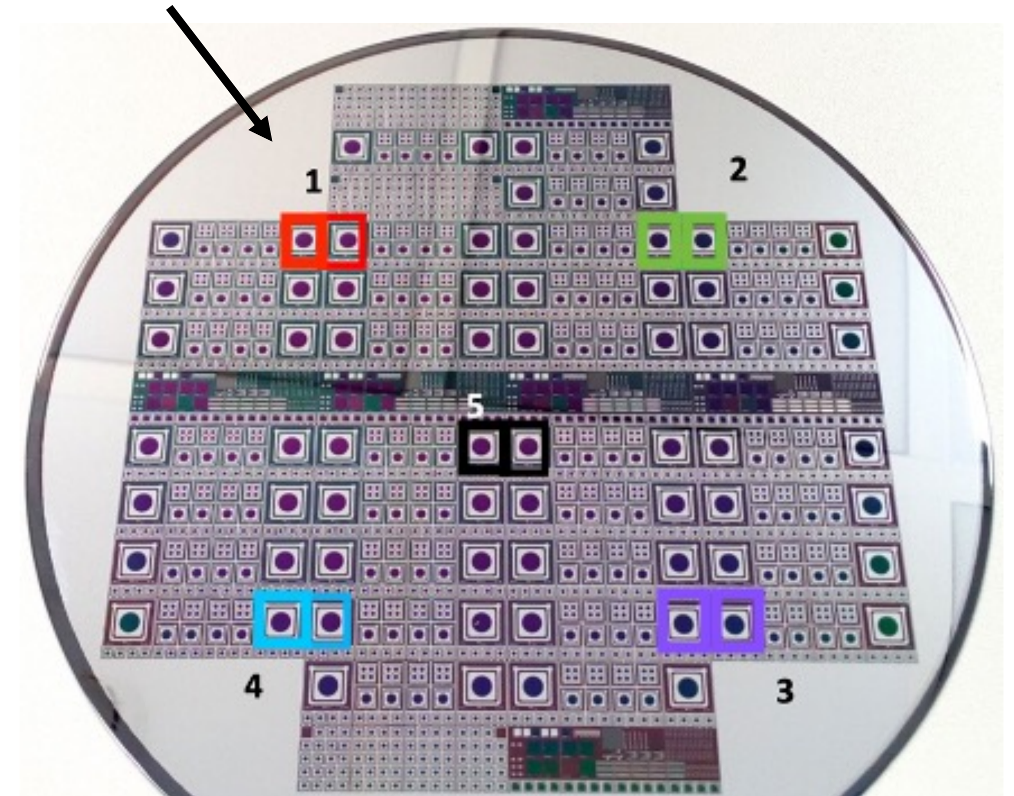

Characterization of wafers – IV data

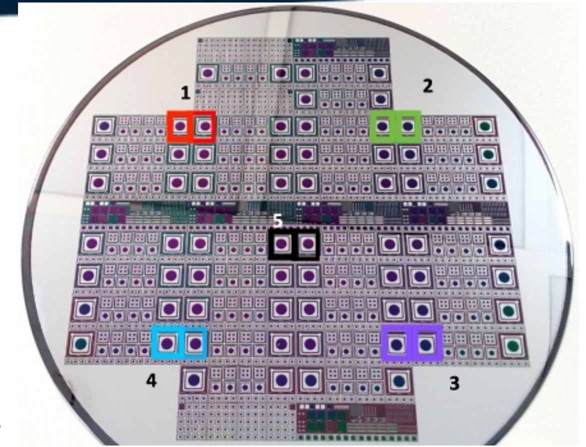

4 mm devices

“soft-breakdown”

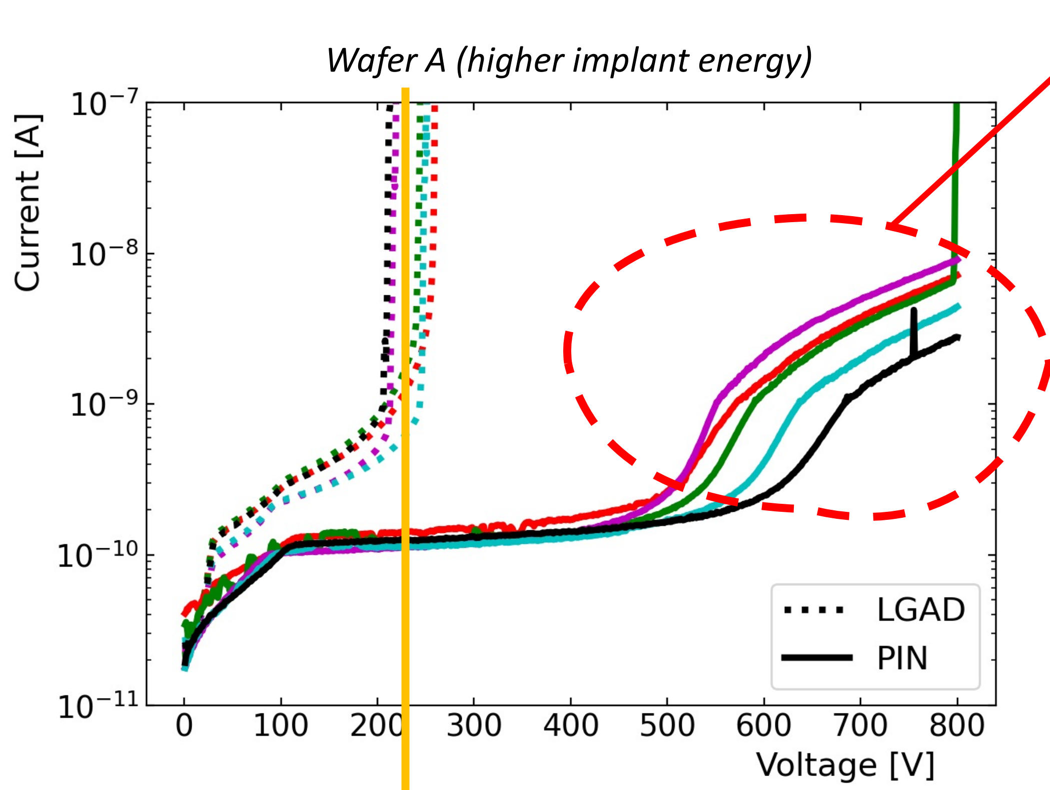

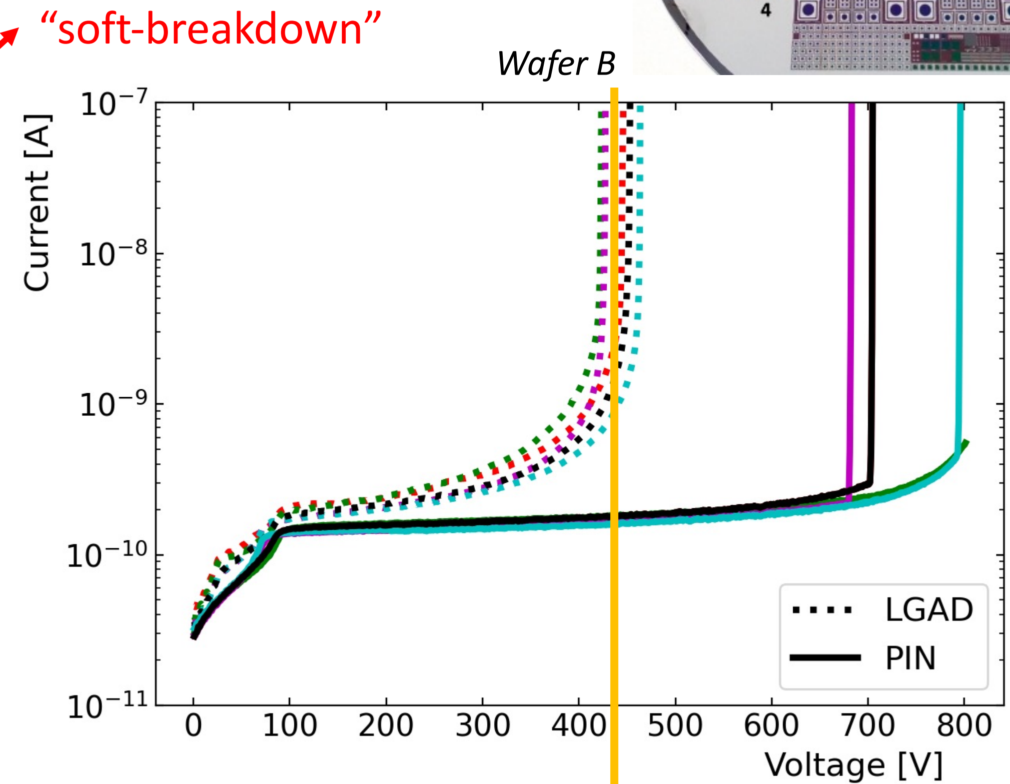

T = 21°C

LGAD breakdown voltage ≈250 V

LGAD breakdown voltage ≈450 V

Characterization of wafers – IV data

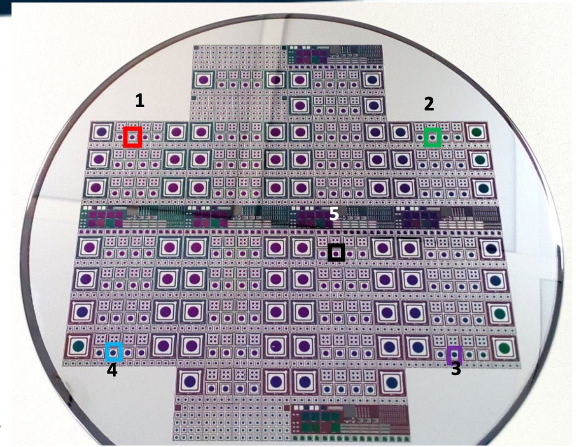

2 mm devices

Wafer A (higher implant energy)

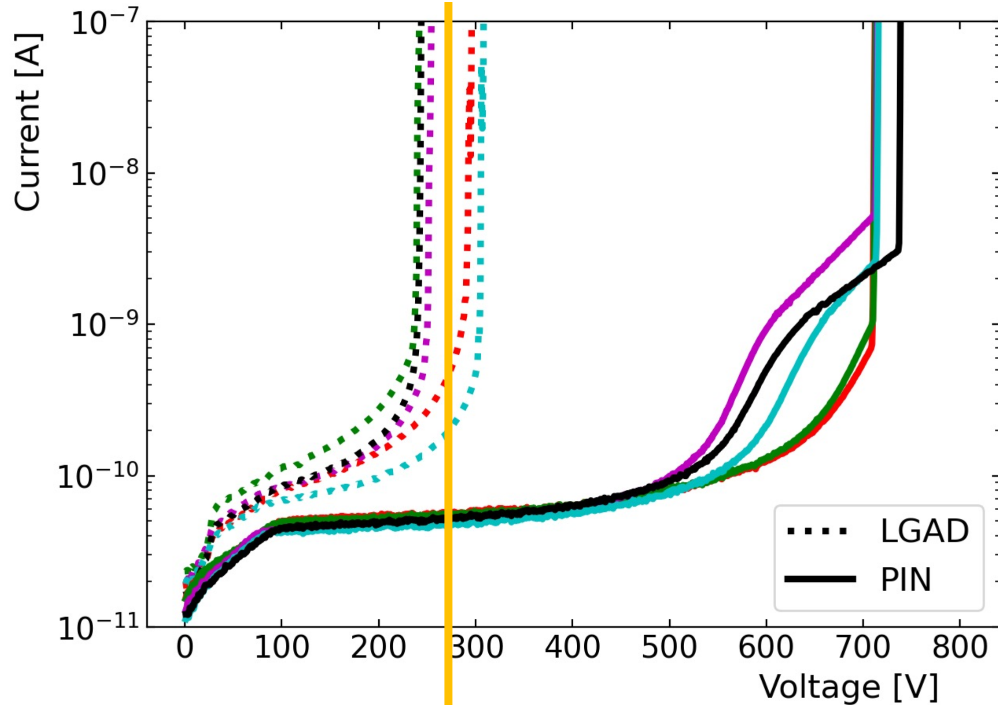

Wafer B

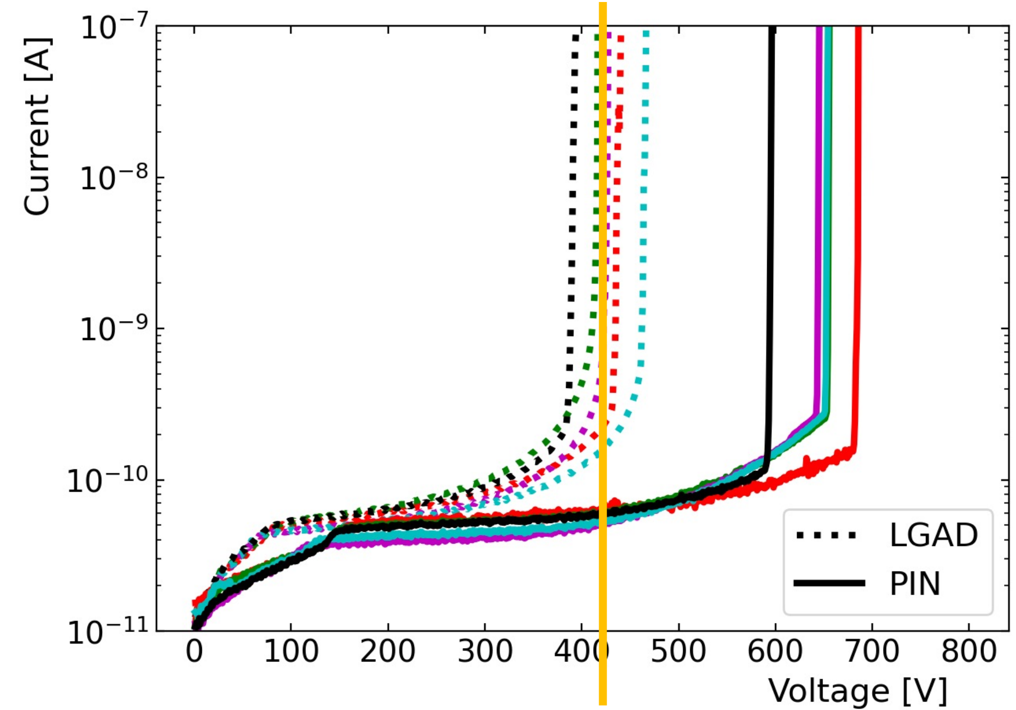

T = 21°C

LGAD breakdown voltage ≈280 V

LGAD breakdown voltage ≈420 V

Characterization of wafers – CV data

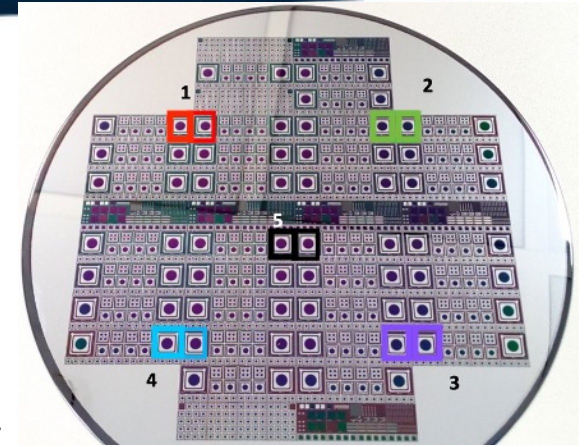

4 mm devices

Wafer A (higher implant energy)

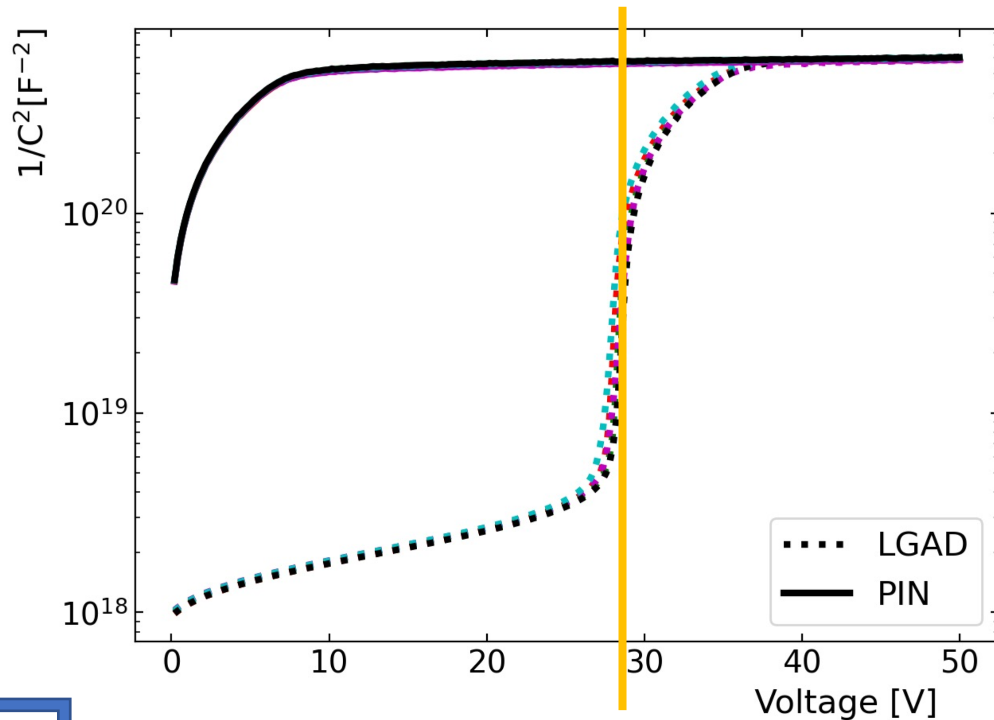

Gain layer depletion voltage ≈30 V

Wafer B

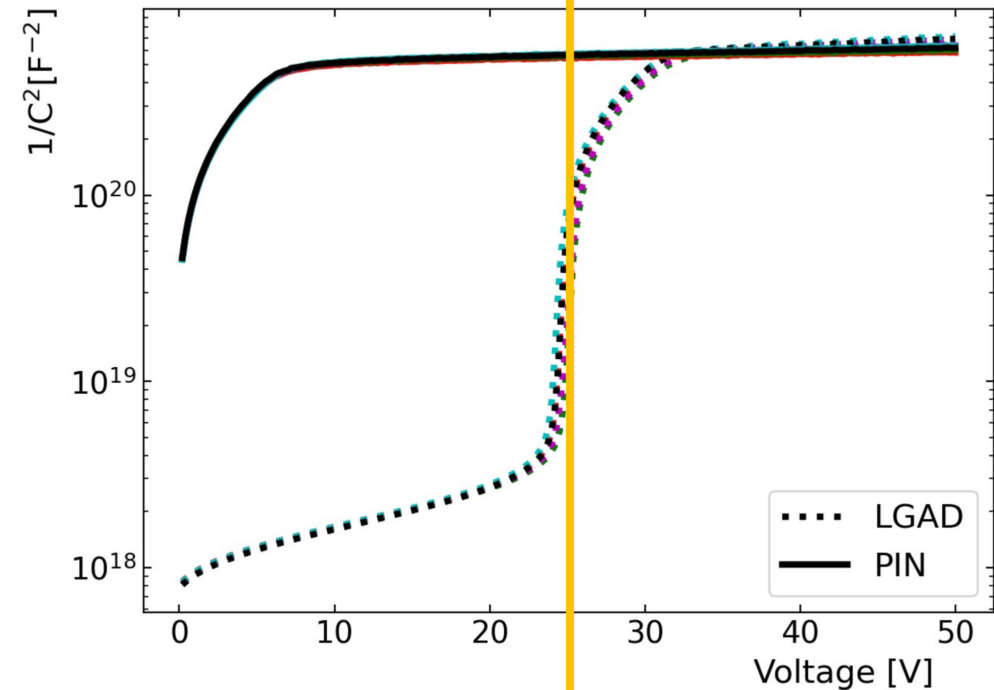

Gain layer depletion voltage ≈25 V

T = 21°C

Characterization of wafers – CV data

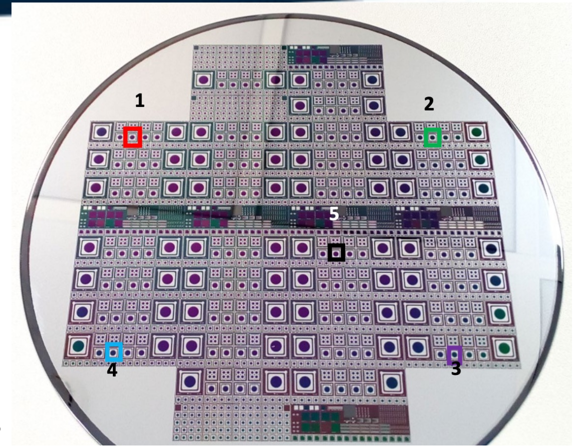

2 mm devices

Wafer A (higher implant energy)

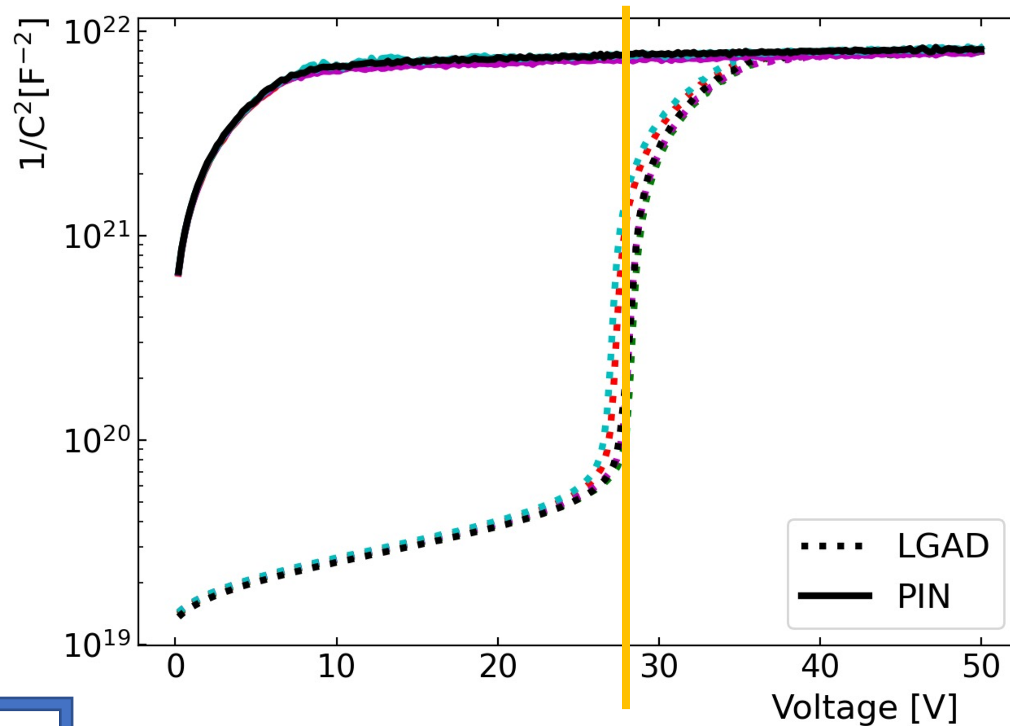

Wafer B

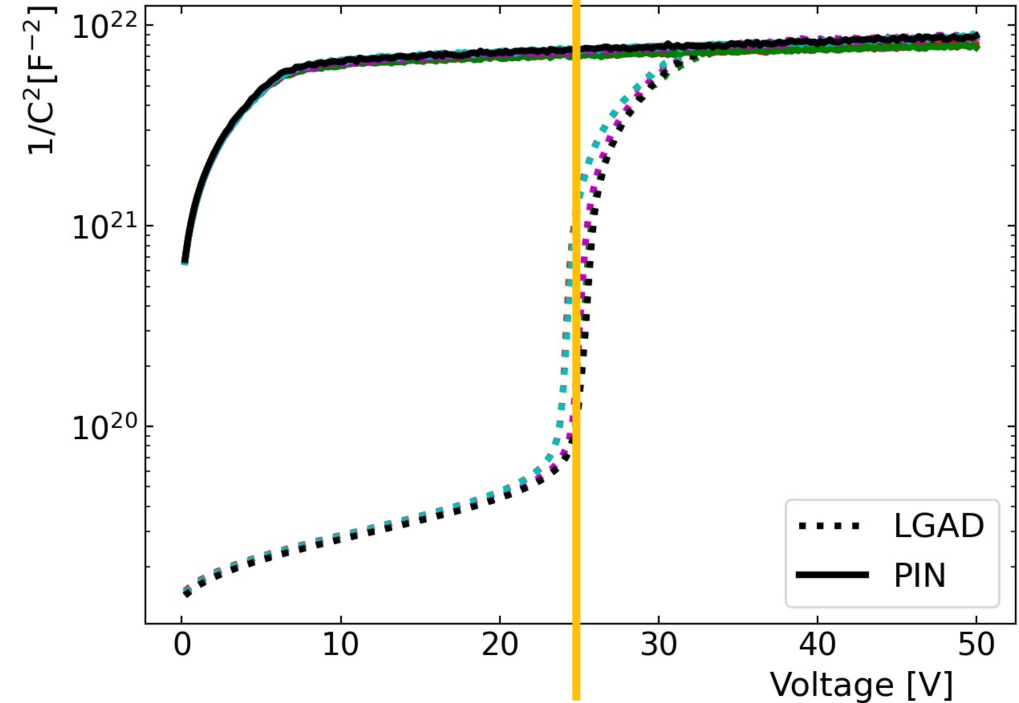

T = 21°C

Gain layer depletion voltage ≈30 V

Gain layer depletion voltage ≈25 V

Concentration inference

- Inferred from capacitance measurement using Profiler’s Equation

Relates to majority carrier density rather than doping

Doping density:

$$\rho = \frac{2}{A^2 e\epsilon\epsilon_0}\left(\frac{d(1/C^2)}{dV}\right)^{-1}$$

at depth (from n^{++} layer):

$$W = \frac{\epsilon\epsilon_0 A}{C}$$

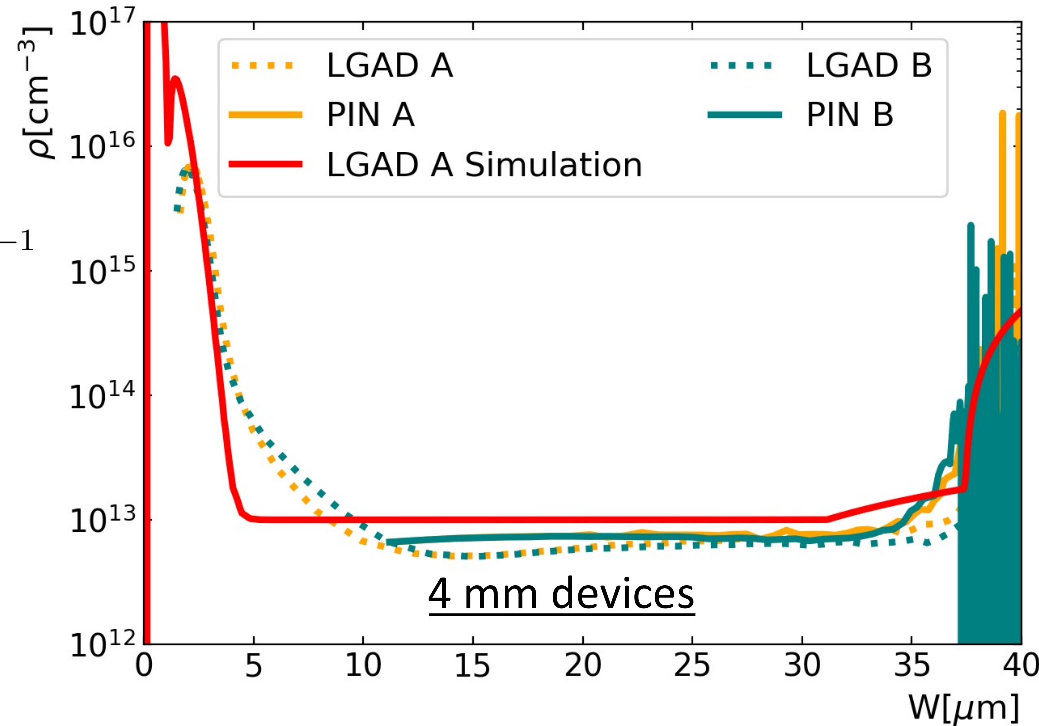

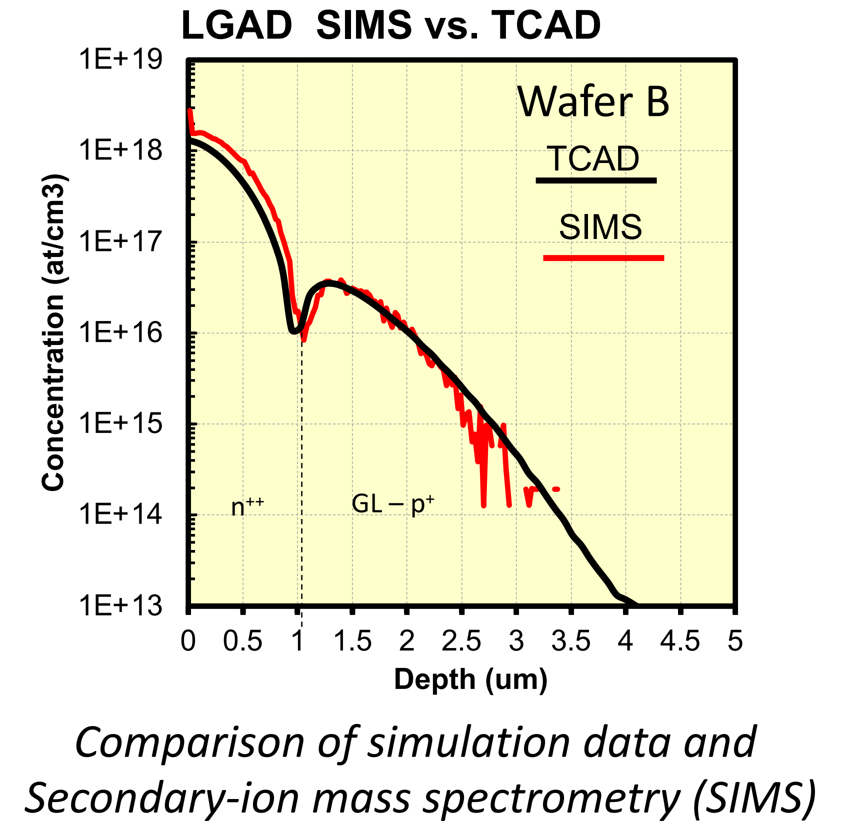

Comparison of simulation data and Secondary-ion mass spectrometry (SIMS)

Laser dicing of wafers

Custom-made 3D printed frame to keep sensors in place and allow for direct comparison pre- and post-dicing

- Laser dicing
  - λ = 1028 nm
  - Power: 10 W
  - Beam size: 25 x 25 um^2

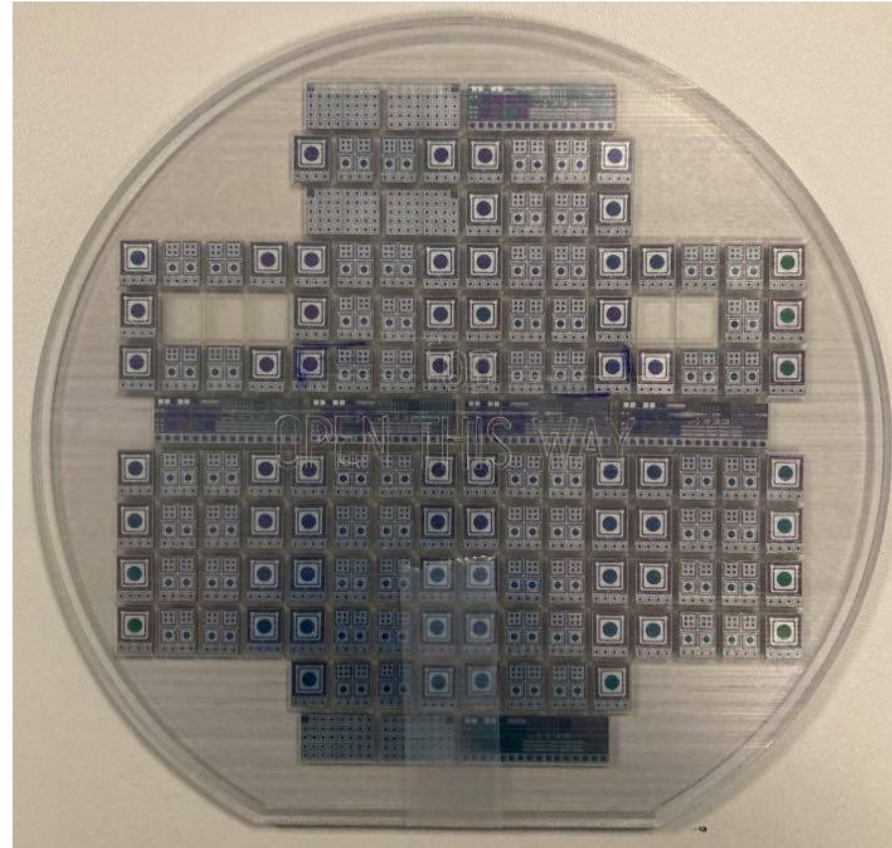

Post-dicing treatment - thermal annealing

- Suspected surface states formed after wafer dicing
  - Detrimental effects: lower breakdown voltage, soft-breakdown behaviour
- Previous behaviour recovered by thermal annealing (conditions: 2 hours at 150°C)

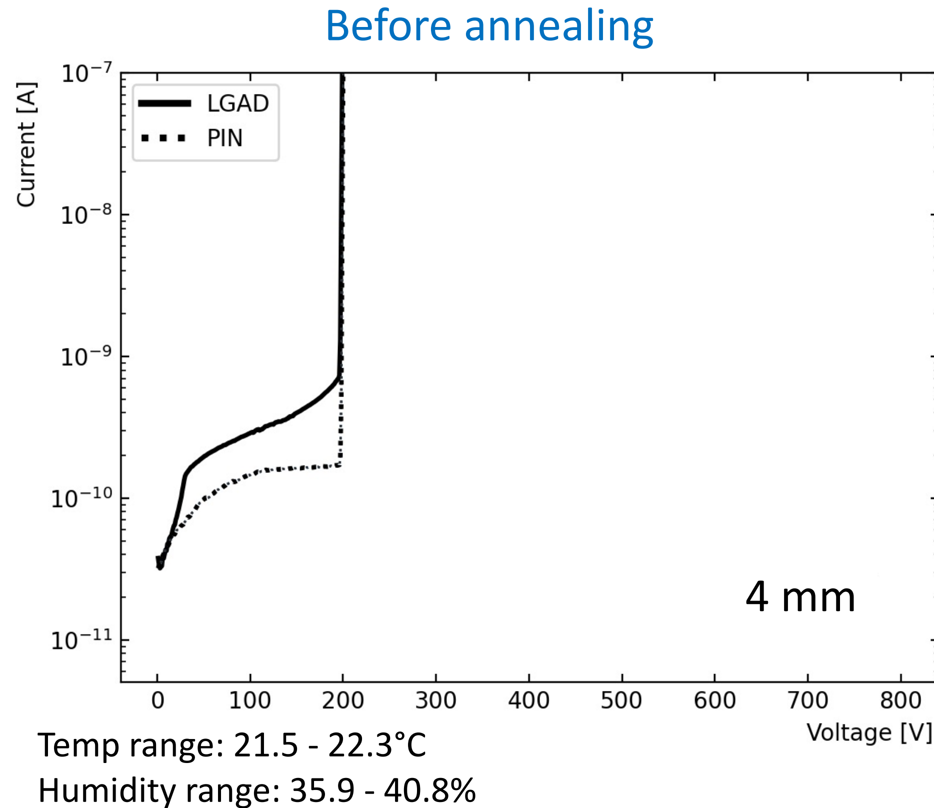

Temp range: 21.5 - 22.3°C
Humidity range: 35.9 - 40.8%

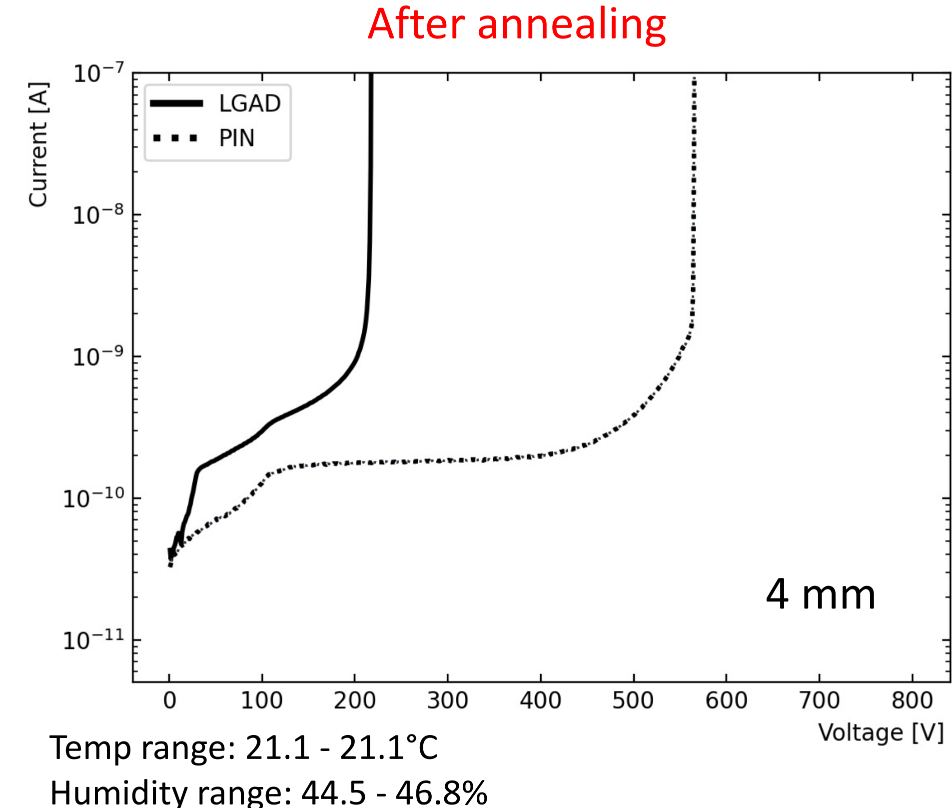

Temp range: 21.1 - 21.1°C
Humidity range: 44.5 - 46.8%

Summary

- Ultra-fast silicon detectors required for 4D tracking and disentanglement of overlapping interactions
- First batch of LGAD devices designed, simulated and produced in collaboration with Teledyne e2v
  - Devices being tested at Oxford, Birmingham and Rutherford Appleton Laboratory
- Observed that higher gain layer implant energy leads to lower breakdown voltage and higher gain layer depletion voltage
- Post-dicing treatment required (thermal annealing)

More on irradiation and gain measurements can be found in the presentation by Jonathan Mulvey @14:45 (CERN time)

Backup – Simulated cross-section

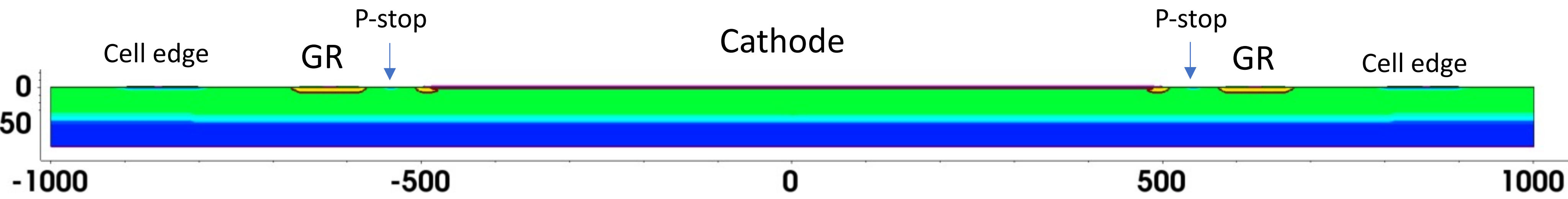

- **2 implantation models implemented:**
  - **MC (1e5 runs) using BCT with modified parameters**
  - **Pearson IV (analytical)**

$$\frac{\Delta E_n}{E_0} = \frac{4M_1M_2}{(M_1+M_2)^2}\cos^2(bI) \quad x\alpha$$

E lost by BC by Nucl. Scattering custom factor α (=1 default)

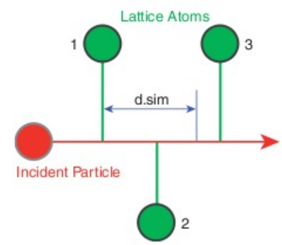

Multi-body collisions for crystal [0.25,1] lattice constant assume d=1

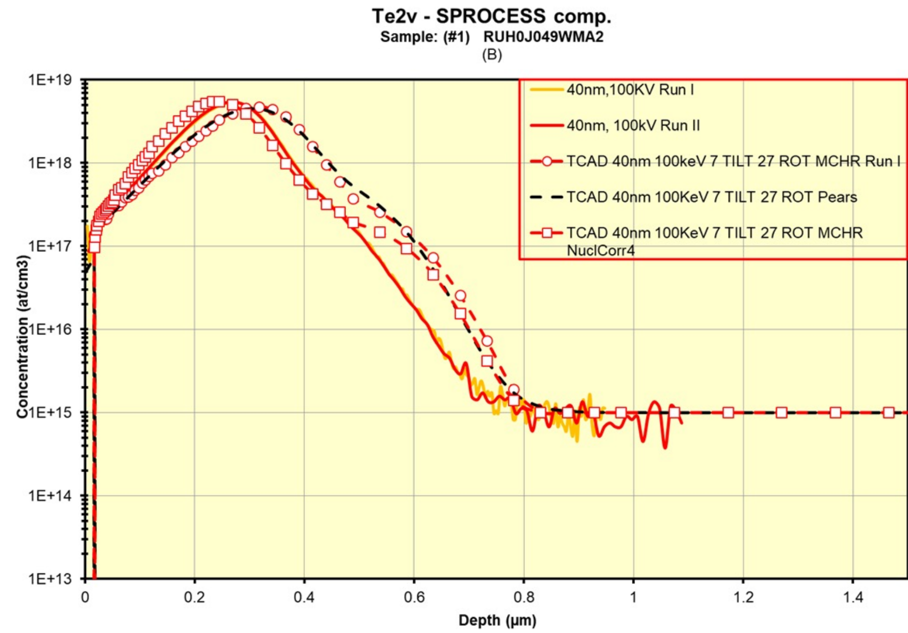

Backup – Traps inclusion

Interface Defect	Level	Concentration	σ
Acceptor	E_C-0.4 eV	40% of acceptor N_{IT} (N_{IT}=0.85·N_{OX})	0.07 eV
Acceptor	E_C-0.6 eV	60% of acceptor N_{IT} (N_{IT}=0.85·N_{OX})	0.07 eV
Donor	E_V+0.7 eV	100% of donor N_{IT} (N_{IT}=0.85·N_{OX})	0.07 eV

* ***Effects of Interface Donor Trap States on Isolation Properties of Detectors Operating at High-Luminosity LHC**, DOI:* 10.1109/TNS.2017.2709815

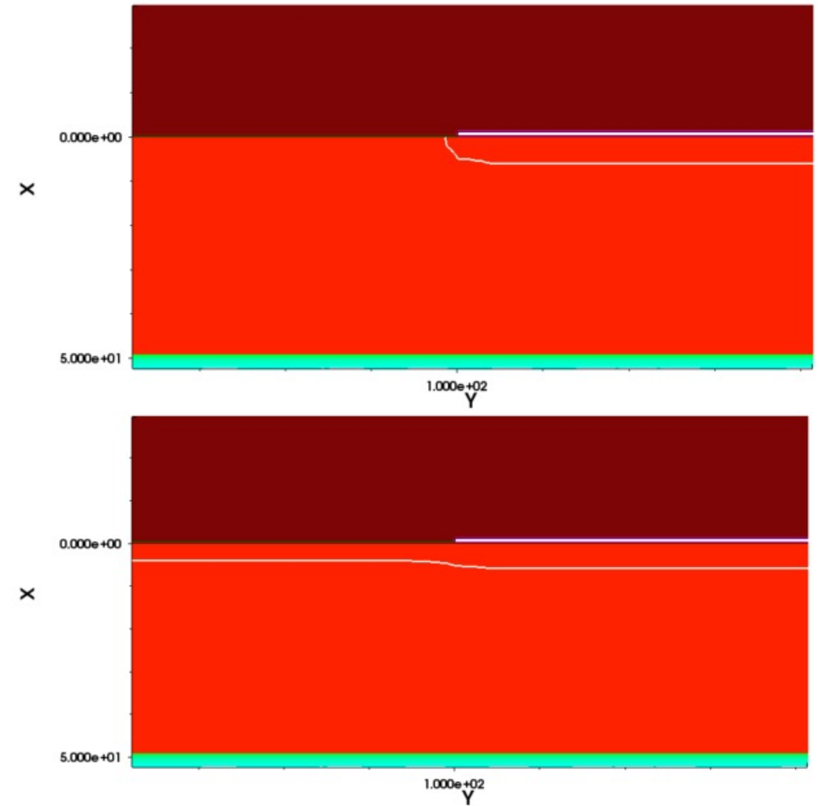

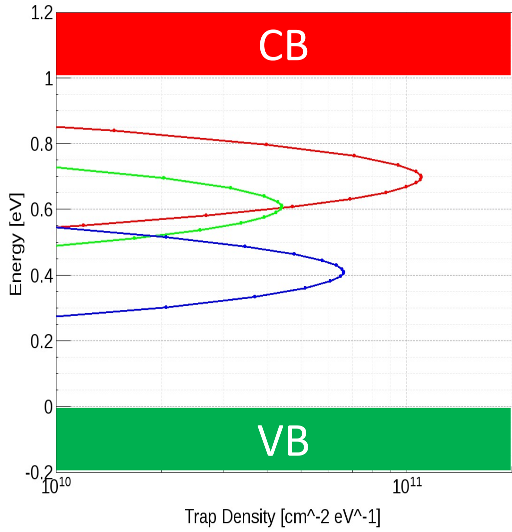

Fixed oxide-charge density and interface traps included
Interface traps distributed among 3 energy levels,
Gaussian , σ = 70 meV
Ratio Oxint/Oxch ~ 0.9

Backup – CV profiling and doping I

- Plots of doping and carriers concentration for WF2 at V_{bias}= 0 V
- HP: x_j:=depletion width
- For $x>x_j$ p concentration differs from doping concentration N_a, due to diffusion
- For $x< x_j$ assume depletion

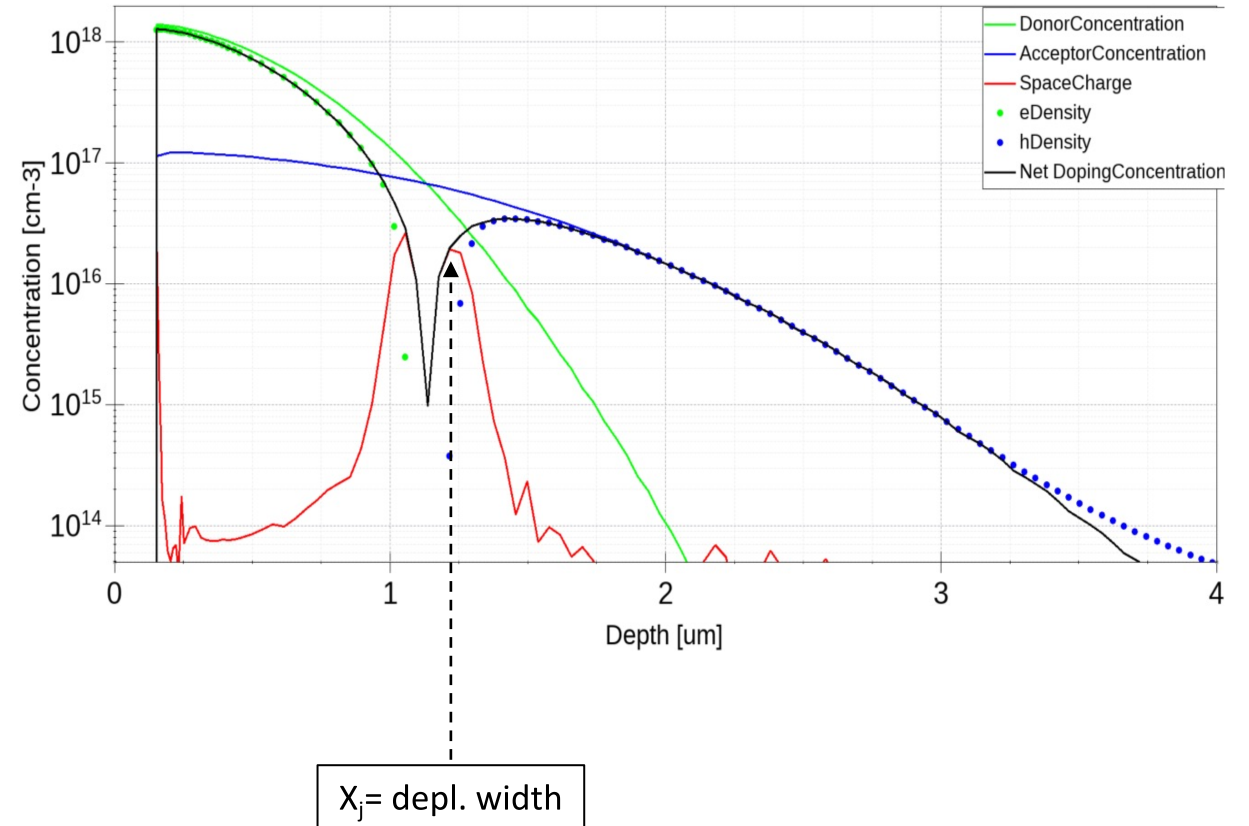

Backup – CV profiling and doping II

Assume:

$$x < x_j : \varrho = -N_A$$

$$x \geq x_j : \varrho = -N_A + p(x)$$

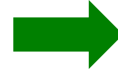

Surface charge and Potential (L = length of the device)

$$Q_s := e\int_0^{x_j} \left(-N_A\right)\,\mathrm{d}x + \int_{x_j}^{L} \left(-N_A + p(x)\right)\,\mathrm{d}x \quad [1]$$

$$\Phi_s := \frac{e}{\varepsilon_s}\left\{\int_0^{x_j} x\left(-N_A\right)\,\mathrm{d}x + \int_{x_j}^{L} x\left(-N_A + p(x)\right)\,\mathrm{d}x\right\} \quad [2]$$

Take differentials from [1] and [2] w.r.t. x_j:

$$dQ_s = e\,p(x_j)\,dx_j$$

$$d\Phi_s = \frac{e}{\varepsilon_s}\,x_j\,p(x_j)\,dx_j$$

$$C_s = \frac{dQ_s}{d\Phi_s} = \varepsilon_s \frac{e\,p(x_j)\,dx_j}{e\,x_j\,p(x_j)\,dx_j} = \frac{\varepsilon_s}{x_j} \quad [3]$$

Assume $\Phi_s \approx V_s$, take derivative of C_s and solve for p in [3]:

$$p(x_j) = \frac{C_s^3}{e\,\varepsilon_s}\left(\frac{dC_s}{d\Phi_s}\right)^{-1}$$

i.e. the usual 'profile equation' showing that what is sampled is p, not N_a